CHAPTER III

INFLUENCE OF DISPERSED-PHASED ELASTICITY ON STEADY-STATE DEFORMATION AND BREAKUP OF DROPLETS IN SIMPLE SHEARING FLOW OF IMMISCIBLE POLYMER BLENDS

[Wanchai Lerdwijitjarud, Anuvat Sirivat, and Ronald G. Larson.,
"Influence of Dispersed-phased Elasticity on Steady-state Deformation and Breakup of Droplets in Simple Shearing Flow of Immiscible Polymer Blends",
in preparation]

INFLUENCE OF DISPERSED-PHASED ELASTICITY ON STEADY-STATE DEFORMATION AND BREAKUP OF DROPLETS IN SIMPLE SHEARING FLOW OF IMMISCIBLE POLYMER BLENDS

ABSTRACT

The effect of dispersed-phase elasticity on steady-state deformation and breakup of isolated droplets for polybutadiene/poly(dimethyl siloxane) blends in simple shearing flow is investigated systematically for values of the dispersed-phase Weissenberg number (Wi_d) ranging up to around 3, where the Weissenberg number is defined as the ratio of the first normal stress difference to twice the shear stress at the imposed shear rate. The dependence on droplet elasticity of steady-state morphology for 10%-dispersed phase blends is also studied. The polybutadiene droplet phase is an elastic "Boger" fluid prepared by dissolving a high-molecular-weight polybutadiene into low-molecular-weight Newtonian polybutadiene. To isolate the contribution of droplet elasticity, all experiments were done on a fixed viscosity ratio of around unity, achieved by adjusting the temperature appropriately for each blend. When the droplet elasticity increases, the steady-state deformation of isolated droplets decreases for fixed capillary number. The critical capillary number for breakup (Ca_{crit}) increases linearly with the Weissenberg number of the droplet phase (Wi_d) up to a value of Wi_d of around unity. When Wi_d is greater than unity, Ca_{crit} seems to approach an asymptotic value of 0.95 for high values of Wi_d. For 10%-dispersed phase blends, the steady-state capillary number (Ca_{ss}) calculated from a volume-averaged droplet diameter is less than the Ca_{crit} for isolated droplets for the same blend. Ca_{ss} increases monotonically with the first normal stress difference of the droplet phase (N_{1d}). Droplet widening in the vorticity direction is not observed even at droplet Weissenberg numbers much in excess of those for which widening is observed in blends of melts, suggesting that widening is strongly influenced by factors other than the first normal stress difference, such as shear thinning or second normal stress differences.

INTRODUCTION

The dispersal of one fluid in another immiscible fluid phase is important in industrial processes, such as emulsion formulation, polymer blending, and also to create interface for heat transfer, mass transfer, and chemical reactions. The size and size distribution of droplets in the matrix phase are crucial for controlling the reactivity of these processes and/or the properties of the final products. For example, the impact strength of a polymer blend is significantly improved when the size of rubbery dispersed-phase inclusions is smaller than a critical value [Wu (1985)]. The droplet size distribution is controlled by deformation, relaxation, breakup, and coalescence of droplets during mixing.

The investigation of deformation and breakup of an isolated Newtonian droplet in an immiscible Newtonian matrix was pioneered by Taylor (1932, 1934). He observed that droplet deformation and breakup of isolated droplets in a Newtonian blend under quasi-steady conditions (i.e., gradually increasing deformation rate) are controlled by two dimensionless parameters, namely the capillary number (Ca), which is the ratio of matrix viscous stress to interfacial stress, and the viscosity ratio (η_r), of the dispersed (η_d) to the matrix phase (η_m). For viscosity ratios near unity, the steady-state three-dimensional shape of an isolated deformed Newtonian droplet sheared in a Newtonian matrix can be represented by an ellipsoid having three different principal axes, the longest of which orients at an angle θ with respect to the flow direction, (Guido and Villone 1998). When the matrix viscous stress ($\eta_m\dot{\gamma}$, where $\dot{\gamma}$ is applied shear rate) overcomes the interfacial stress (Γ/r_0, where Γ and r_0 are the interfacial tension and the undeformed droplet radius, respectively), the droplet will break. This occurs when the ratio of the viscous to the interfacial stress which is the capillary number $Ca \equiv \eta_m\dot{\gamma}r_0/\Gamma$ exceeds a critical value, Ca_{crit}. Ca_{crit} is a minimum when η_r is around unity [Grace (1982); De Bruijn (1989)]. The flow type (shear vs. extensional flow) was also found to effect the correlation between Ca_{crit} and η_r [Rallison and Acrivos (1978), Bentley and Leal (1986)].

For polymer blends, non-Newtonian behavior, including elasticity and shear-thinning, is expected to influence the deformation and breakup of droplets. Wu (1987) studied the steady-state average droplet size in extruded viscoelastic polymer blends containing 15% of dispersed phase and compared the results with those of Newtonian blends. Like the Newtonian blend, the minimum in Ca for these polymer blends was found at a viscosity ratio of around unity; however the value of Ca at η_r = 1 for Wu's polymer blends was around ten times greater than that of a Newtonian system. Many experimental results on immiscible viscoelastic blends when either one phase or the other is viscoelastic have been reported in the literature [Flumerfelt (1972); Elmendrop and Maalcke (1985); Milliken and Leal (1991); Tretheway and Leal (2001)]. An unusual phenomenon, transient and steady-state droplet widening along the vorticity axis [Levitt et al. (1996); Hobbie and Migler (1999); Migler (2000); Mighri and Huneault (2001)], was observed for a viscoelastic droplet sheared in a viscoelastic matrix.

Most of the experimental evidence shows that elasticity of the droplet fluid inhibits droplet deformation, causing the droplet to break at a higher capillary number, while elasticity of matrix phase tends to destabilize the droplet, making it break at a lower capillary number. However, quantitative correlations between Ca and elasticity of droplet or matrix phase are rare. Varanasri et al. (1994) studied the breakup of isolated viscoealstic droplets sheared in purely viscous Newtonian fluids in a cone-and-plate device and found a linear relationship between Ca_{crit} and the first normal stress difference of the dispersed phase fluid at a fixed viscosity ratio. However, there existed a critical value of viscosity ratio, η_r^*, above which the viscoelastic droplet was easier to break than the purely viscous droplet. The reasons for these results are still unclear. Mighri et al. (1998) investigated the deformation and breakup of isolated droplets under a simple shear flow for a blend prepared from "Boger" fluids (in which each blend component is a dilute polymer in a Newtonian matrix) and also constructed a correlation between Ca_{crit} and elasticity contrast, as measured by the ratio λ_d/λ_m of the relaxation time of the droplet phase ($\lambda_d \equiv N_{1d}/2\eta_d\dot{\gamma}^2$) to that of matrix phase ($\lambda_m \equiv N_{1m}/2\eta_m\dot{\gamma}^2$), where N_{1d} and N_{1m} are the first normal stress differences of dispersed and matrix phase, respectively. The

correlation between Ca_{crit} and λ_d/λ_m was found to be nonlinear, in which Ca_{crit} sharply increased with increasing λ_d/λ_m when $\lambda_d/\lambda_m < 4$, but for $\lambda_d/\lambda_m > 4$, Ca_{crit} reached an asymptotic value of Ca_{crit} around 0.9.

In most previous work, both droplet elasticity and viscosity ratio were varied simultaneously. However, the study of droplet behavior when droplet elasticity is the sole manipulated valuable has been recently reported [Lerdwijitjarud *et al.* (2003)]. In this work, the deformation and breakup of isolated droplets of weakly elastic fluid ($Wi_d \leq 0.02$, $Wi_d \equiv(\Psi_{1,d}/2\eta_d).\dot{\gamma}_c$; where $\Psi_{1,d}$ is the first normal stress difference coefficient of dispersed phase) sheared in a Newtonian matrix were microscopically investigated at a fixed viscosity ratio of unity. Elasticity of the droplet produced a reduction in the degree of deformation at any given imposed Ca, and correspondingly resulted in greater value of Ca_{crit} for droplet breakup compared with a Newtonian droplet. The breakup mechanism appeared to be similar to that in a Newtonian fluid; i.e., the droplet deformed increasingly in the flow direction as the shear rate was gradually increased, until breakup occurred. A quantitative relationship linking Wi_d to Ca_{crit} was established. Ca_{crit} increased linearly with increasing Wi_d, but a downward deviation from linearity was found for the blends with highest Wi_d, i.e., for $Wi_d \approx 0.02$.

This paper is devoted to finding a quantitative relationship between the critical capillary number for breakup, Ca_{crit}, and elasticity of dispersed phase, as measured by Weissenberg number, Wi_d, for the blend systems with a fixed viscosity ratio of unity and a much higher degree of droplet phase elasticity than in our previous work [Lerdwijitjarud et al. (2003)], in order to move toward more realistic commercial high-molecular-weight polymer blends with high elasticity.

EXPERIMENTAL

A. Materials

The materials used as the matrix and dispersed phases of the blends in this study were polydimethylsiloxane (PDMS) (Viscasil 100M donated by General Electric) and low-molecular-weight, Newtonian, polybutadiene (PBd) (Startomer R150 donated by Startomer Inc.), respectively. The properties of both fluids are listed in Table 3.1. A high-molecular-weight polybutadiene (M_w = 1.43 x 10^6, M_w/M_n ~ 1.13) was also used as a flexible polymer component added to the low-molecular-weight PBd to make "Boger" fluids with elasticity but low shear thinning [Boger and Binnington (1977)].

B. Blend Preparation and Characterization

To remove all volatile components, both PDMS and PBd were placed in a vacuum oven at 50 ^{0}C until no further weight change was observed. The polybutadiene "Boger" fluids were prepared by thoroughly dissolving high-molecular-weight polybutadiene into methylene chloride. The solution was gently mixed with low-molecular-weight PBd by rolling-bottle technique at ambient condition for at least 7 days to ensure that a homogeneous solution was achieved. The mixture was then vacuum dried at 50 ^{0}C to eliminate the methylene chloride and other volatile materials until the weight loss ceased. The weight percentages of high-molecular-weight flexible polymer in the polybutadiene "Boger" fluid for this work are 0.1, 0.2, 0.5, and 1.0. The steady-state viscosities and first normal stress differences, N_1, of all fluids were measured by a cone-and-plate rheometer with 25-mm. plate diameter and cone angle of 0.1 rad. (Rheometrics Scientific, ARES). The temperature at which both PDMS and low-molecular-weight PBd have the same viscosity is 18.3 ^{0}C. At this equiviscosity temperature of these two fluids, the PBd shows Newtonian behavior at shear rates of 0.1-10 s^{-1}, whereas weak shear thinning and a small value of N_1 at high shear rates are observed for PDMS (see Figure 3.3a). Figure 3.1 depicts the dependence of steady-state viscosity and N_1 of all PBd

"Boger" fluids on shear rate at a temperature of 18.3 ^{0}C. The zero-shear viscosities, η_0, and also the elasticities, as measured by the N_1 values, of the "Boger" fluids increase with increasing concentration of high-molecular-weight polymer component in the solution. Unfortunately, shear thinning also increases with increasing concentration of long-chain species, which is especially evident in the "Boger" fluids containing the high-molecular-weight PBd at concentrations of 0.5% and 1.0%. The dependence of η_0 on weight percent of long-chain polymer in PBd "Boger" fluid is shown in Figure 3.2. For the "Boger" fluids containing 0.1%, and 0.2% of long-chain polymer, the solutions are believed to be dilute in high-molecular-weight PBd because we observe an approximately linear relation between the concentration of high-molecular-weight polymer and the increment in zero-shear viscosity over that of low-molecular-weight PBd. However, the linear relation is no longer valid for the solutions containing 0.5%, and 1.0% of high-molecular-weight polymer, evidently because of the onset of entanglements at these higher concentrations.

The blends used in this study are presented in Table 3.2. To clearly isolate the contribution of elasticity, the viscosity ratios of the blends were fixed at around unity. The testing temperature, therefore, was varied from blend to blend to compensate for the effect of long-chain polymer on the viscosity of PBd dispersed phase. For A0, A1, and A2 blends, the viscosity ratios could be set to around unity using only a single value of temperature for each blend (see Figure 3.3). Due to the shear-thinning characteristics of the 0.5% and 1.0% high-molecular-weight PBd solutions, however, different testing temperatures were used for these blends over different ranges of shear rate to better satisfy the equiviscosity condition (see Figures 3.4 and 3.5). The steady-state viscosities and the first normal stress differences of the PDMS matrix and the PBd dispersed phase at the temperature at which both phases have the same viscosity are shown for all blends in Figures 3.3, 3.4, and 3.5. The viscosity ratios of all blends were well controlled to be unity $\pm$ 5% at the testing conditions, whereas the elasticity of the dispersed phase monotonically increases with concentration of high molecular weight Pbd in blends A0, A1, A5, A10, as indicated by the increasing values of N_1 of the droplet fluid.

C. Experiments on Isolated Droplets

1. Instruments and sample loading

An optical flow cell (Linkam CSS450, Linkam Scientific Instruments Inc.), consisting of two parallel quartz disks, i.e. a rotatable lower one and a fixed upper one, mounted on an optical microscope (Leica DMRXP, Leica Imaging Systems Inc.) was used to conduct the experiments. The temperature of the flow cell was controlled by the cell-heating elements and circulating water from a water bath. Images were captured by a CCD camera (Cohu 4910, Cohu Inc.) in the flow-vorticity plane and transferred to a PC computer via a frame-grabber card (LG3-128, Scion Corporation Inc.). The images were analyzed by the Scion Image software.

The PDMS matrix phase was loaded into the flow cell, and the fluid was allowed to level. Several PBd droplets were then immersed into the matrix using a small needle. The upper plate of the flow cell was gradually lowered until the quartz disk touched the sample and the desired gap was reached. For the experiments on isolated droplets, the total amount of dispersed phase in the blend was less than 0.2%.

II. Optical microscopy of an isolated droplet

Droplets located near the center of the gap and separated from their neighboring droplets by a distance more than three times the diameter of the biggest neighboring droplet were considered to be isolated droplets and were chosen for observation and measurement. Since hydrodynamic interactions with the solid surfaces disappear if the distance between the closest surface and the droplet center is more than five times the droplet radius [Kennedy et al. (1994); Uijittewaal and Nijhof (1995)], the gap in all our experiments was at least ten times larger than the diameter of the chosen droplet. Since the images of the deformed droplet were taken only in the flow-vorticity plane, which is the plane perpendicular to the shear gradient direction, the lengths of all three principle axes of the ellipsoidal droplet could not be obtained unless the orientation angle (θ), the angle between the major axis of deformed droplet in the flow-flow gradient plane, was known. This

orientation angle can be predicted from either the affine deformation model for step strains or Chaffey and Brenner relation for steady-state shearing [Chaffey and Brenner (1967)]. For a step-strain or startup flow experiment, if the imposed Ca is at least three times higher than Ca_{crit}, the orientation angle predicted from the affine deformation model has been found to be close to the experimental value obtained from microscopy for both Newtonian and viscoelastic blends in experiments that imaged the droplet from two different directions [Yamane et al. (1998); Okamoto et al. (1999)]. For $Ca \leq Ca_{crit}$, Chaffey and Brenner (1967) found that for isolated Newtonian droplet sheared in immiscible Newtonian matrix, the orientation angle of the steady-state deformed droplet depended on the applied Ca and the viscosity ratio of the system. Guido and Villone (1998) compared the predictions of the Chaffey and Brenner relation with the experimental results obtained from microscopy for polydimethylsiloxane droplets sheared in polyisobutylene at η_r of 1.4 and 2, and found good agreement between the two.

III. Interfacial tension determination

The interfacial tensions of all blend systems studied were determined by the deformed-droplet retraction technique [Luciani et al. (1997); Guido and Villone (1999); Mo et al. (2000); Xing et al. (2000)]. The shape evolution of a deformed isolated droplet during relaxation from an ellipsoidal back to a spherical shape was recorded. The characteristic relaxation time for an isolated droplet, τ, can be obtained from the slope, $-1/\tau$, of a straight line fit to the data in the linear relaxation regime of semilogarithemic plots of the deformation parameter, Def., versus relaxation time. The interfacial tension, Γ, can be calculated from the Palierne Model [Palierne (1990); Graebling et al. (1993)] in the limit of zero volume fraction of the dispersed phase:

$$\tau = \frac{(3 + 2\eta_{r,0})(16 + 19\eta_{r,0})r_0\eta_{m,0}}{40(1 + \eta_{r,0})\Gamma}$$

where $\eta_{r,0} \equiv \eta_{d,0}/\eta_{m,0}$ is the ratio of zero-shear viscosities of dispersed to matrix phase, and r_0 is the radius of the spherical drop. For viscoelastic systems, the contribution of both droplet and matrix elasticity to the relaxation of the droplet

shape may lead to errors if this equation is used. However, the relation can still be used to determine the interfacial tension of viscoelastic materials if the relaxation of the nonNewtonian elastic stress of the blend constituents is relatively fast compared with the droplet shape relaxation and the droplet retraction rate is sufficiently slow to ensure that the materials behave as Newtonian during the droplet shape relaxation [Luciani *et al.* (1997), Xing *et al.* (2000)]. For large enough droplets, relaxation should become slow enough that viscoelastic stresses relax too quickly to influence droplet shape relaxation and hence the rate of relaxation is then governed by the interfacial tension alone. In this study, the interfacial tension values obtained using the Palierne formula applied to experiments on 180-μm and 100-μm droplets are the same within an experimental error for all blend systems, which implies that the true interfacial tension was obtained. The interfacial tension of all blends is presented in Table 3.2.

IV. Steady-state deformation and breakup of isolated droplet

For a steady-state deformation experiments, a suitable isolated droplet with desirable size was selected. The chosen droplet was then driven out of the field of view by applying a relatively small shear rate until the desired magnitude of the strain to be subsequently imposed strain was reached. The shear flow was stopped to allow the droplet to completely relax into a spherical shape. The same strain in the opposite direction was then applied at the desired shear rate, thus deforming the droplet and simultaneously bringing it back into viewing window. The droplet images were recorded by using a CCD camera at the maximum capturing speed (25 frames/ second). The capturing process was begun before the sheared droplet moved into the viewing window and continued until the shear flow was stopped and the deformed droplet started to relax. To ensure that a steady-state deformation was established, the strain required to reach a steady-state droplet shape was determined. After determining the steady-state shape at a fixed shear rate, the applied shear rate was gradually increased from low to high in small incremental steps until the critical shear rate required for breaking the droplet was reached. The same procedure was applied to the isolated droplet with smaller sizes.

D. Experiments on Concentrated Blends

The concentrated blend compositions are 10% by weight of PBd dispersed phase and 90% by weight of PDMS matrix phase. The blend constituent components were weighed and mixed together with a spatula for around 20 min. resulting in a white-creamy product. The sample was placed in the vacuum oven at room temperature for about 1 hr to remove all bubble generated during the mixing step. The bubble-free sample was loaded into the flow cell. The upper plate of the flow cell was gradually reduced until the gap reached 500 microns. The testing temperature was set to a value at which both the matrix and dispersed phases have the same viscosity. After the loading process, the sample was pre-conditioned by shearing at a shear rate of 0.3 s^{-1} for a strain of 20,000 units. During this step, coalescence clearly dominated leading to a relatively coarse morphology.

After pre-conditioning process, the shear rate was stepped up to 0.5 s^{-1}. A strain of 20,000 units was used to ensure that the steady-state morphology at this shear rate was reached. The flow was then stopped to allow the deformed droplets to relax back into spherical shapes. Due to the high viscosity of the matrix fluid and low temperature of our blend systems, the diffusion coefficient associated with Brownian motion of the droplets is small ($\sim 10^{-6}$ $\mu m^2/s$ for droplets with diameter of 5 μm at 20 ^0C). Thus, the coalescence effect should be negligible in quiescent blends since the time waiting for droplet relaxation is less than 30 s. The blend images were then captured. The shear rate was subsequently increased in small steps, i.e. 0.7, 1.0, 2.0, 3.0 and 5.0 s^{-1}, from the previous steady-state shear rate. For each shear rate, a strain of 20,000 was allowed to attain a steady-state morphology before capturing images.

The blend images were transferred to a Photoshop program (Adobe Systems, Inc) to outline the droplets. The images were brought back to the Scion-Image software to determine the droplet diameter. From the droplet size distributions, the volume-average droplet diameter, D_v, was calculated by using the following equation:

$$D_v = \sum_i \Phi_i D_i$$

where Φ_i is the volume fraction of the droplets with diameter D_i relative to the total volume of the droplets. Typically, data from 400-600 droplets were used to calculate D_v.

RESULTS AND DISCUSSION

A. Steady-State Deformation and Breakup of Isolated Droplet

Newtonian Blend System

When a steady shear flow is applied to an isolated spherical droplet, the droplet simultaneously moves and deforms. If the imposed shear rate is less than the critical shear rate for droplet breakup, a steady-state deformed droplet shape is eventually obtained after sufficient strain. The strain required to reach a steady-state deformation shape increases with increasing applied shear rate and droplet size. For Newtonian droplets sheared in Newtonian matrix at viscosity ratios near unity, Guido and Villone (1998) verified that the steady-state deformed shape of the droplet can be approximated as an ellipsoid having three different principle axes, i.e. a is the major axis of the ellipsoid oriented at a particular angle (θ) within a flow-gradient plane, b is the minor axis in the shear-gradient direction, and c is the minor axis in the vorticity direction.

Figure 3.6a shows the dependence of the steady-state shape of the droplet in terms of deformation parameter, Def $\equiv (a-b)/(a+b)$, on the imposed capillary number for blend A0 (low-molecular-weight PBd/PDMS blend), for various droplet sizes, i.e. 180 μm ± 10%, 100 μm ± 10%, 50 μm ± 10%, and 20 μm ± 10% in diameter. As depicted in Figure 6a, the curves for all droplet sizes coincide well with each other, and are also close to Taylor's prediction (Def = Ca $[(19\eta_r+16)/(16\eta_r+16)]$). The last data point in each curve can be estimated to be the critical point above which the steady-state deformed shape no longer exists and droplet breakup finally occurs. The critical capillary number, Ca_{crit}, for droplet breakup for blend A0 is equal to 0.50 for droplets with diameter of 180μm ± 10%, 0.52 for diameter of 100μm ± 10%, 0.51 for diameters of 50μm ± 10%, and 0.54 for diameters of 20μm ± 10%. The value of Ca_{crit} obtained from Taylor's prediction is 0.5, which is similar to our results. The good agreement of our results on blend A0 with Taylor's prediction is obtained in both the dependence of Def. on the imposed Ca, and in the value of Ca_{crit} for droplet breakup.

Effect of Dispersed-phase Elasticity on Steady-state Droplet Deformation and Breakup

As in the A0 blend containing Newtonian components, for the A1 blend containing isolated slightly elastic droplets, the dependence of the deformation parameter on capillary number for was the same for various droplet sizes, as shown in Figure 3.6b. although the capillary number at which breakup occurs monotonically increases with decreasing droplet size. For the A5 blend, however, as shown in Figure 3.6c, the droplet diameter influences both the capillary number at breakup and the deformation before the breakup condition is reached. . As shown in Figures 3.6b, and 3.6c, Ca_{crit} monotonically increases with decreasing droplet size for blends A1 and A5. In order to obtain the same value of Ca for a given blend, the applied shear rate has to be higher for a smaller droplet and the degree of elasticity also increases with increasing shear rate. Thus, at the same Ca, the smaller droplet has a higher elasticity, leading to a higher shear rate required for breakup.

To better characterize this elastic effect, the correlation between Def and the imposed Ca for different blends having comparable droplet sizes is plotted on the same graph in Figure 3.7. For each droplet size, the more elastic droplet deforms less and Ca_{crit} for droplet breakup increases with increasing droplet elasticity. The degree of elasticity of the fluid can be represented by a Weissenberg number (Wi), a ratio of elastic stress to viscous stress. Therefore, we try to determine a quantitative correlation between the Weissenberg number of droplet fluid, $Wi_d(\dot{\gamma}) = [\Psi_{1d}(\dot{\gamma})/2\eta_d(\dot{\gamma})].\dot{\gamma}$, and Ca_{crit} for droplet breakup. We obtain the values of the first normal stress difference coefficient, Ψ_1, directly from the measured N_1 or from extrapolated values, if breakup occurred at a shear rate too low to accurately measure the value of N_1. The relationship between Wi_d and Ca_{crit} obtained in this way is shown in Figure 3.8a, where the closed symbols represent the data obtained from the directly measured N_1 value and the open symbols represent data from extrapolated N_1 values. It should be noted that the shear rate inside the droplet is in general different from the imposed shear rate; it is not uniform and depends on the shape of

deformed droplet. The N_1 value inside the droplet, thus, will not be uniform and will be a complex function of shear rate and droplet size. However, for simplicity, we used the nominal N_1 values at the imposed shear rate to calculate Wi_d. As shown in Figure 3.8a, Ca_{crit} increases linearly with Wi_d up to a value of Wi_d of around 1.0. Interestingly, the Ca_{crit} value of 0.5 is obtained from the extrapolation of the linear regression line to Wi_d equal to zero, which recovers the droplet breakup condition from Taylor's prediction for Newtonian blend. When Wi_d is greater than unity, a downward curvature from linearity is observed, and the Ca_{crit} seems to reach a constant value of 0.95 for a high value of Wi_d. Surprisingly, the asymptotic value of Ca_{crit} of our results is close to the value of Ca_{crit} around 0.9 (or 1.8 in the plot of $\eta_m\dot{\gamma}_{crit}D/\Gamma$ versus λ_d/λ_m) reported by Mighri *et al.* (1998). The general conclusion drawn from Figure 3.8a is that the elasticity of the droplet resists deformation of the droplet; however the effect seems to saturate at a value of Ca_{crit} around 0.95 for high values of Wi_d. However, another possible reason for saturation in Ca_{crit} is the shear-thinning behavior of the dispersed phase fluids because all the data at Wi_d above unity are obtained from blend system A5 and A10, both of which have dispersed phase fluids with shear-thinning behavior (see Figures 3.4, and 3.5).

Figure 3.8a also includes data from our earlier study (Lerdwijitjarud et al. 2003), which was limited to a droplet Weissenberg number no higher than 0.02, because of the lower molecular weight of the high-molecular-weight Pbd component in the Boger fluid used in that study. Figure 3.8b shows the same data with a logarithmic x axis.

We note that although our blends contained elastic droplets with Wi_d up to around 3, all droplets stretched and broke in flow direction similar to that of Newtonian droplets for all experimental conditions studied. Steady-state droplet vorticity widening (or "vorticity stretching") was not observed in our experiments. Table 3.3 shows the rheological data for blend systems in this studied compared with those data taken from literature that reported steady-state vorticity stretching of droplets. From Table 3.3, it seems that we need Wi_d greater than 20 to get steady-state droplet widening in the vorticity direction for blends of "Boger" fluids, which is beyond the range of Wi_d studied here. For blends of high-molecular weight polymer *melts*, however, droplet widening has been detected at Wi_d somewhat lower than

unity. Another relevant point is that the minimum capillary number for which widening occurs has been reported is around 7, which is much greater than the critical capillary number for droplet breakup of the blends studied here. We also point out that the viscosity ratio has been found to play an important role in droplet widening, and this parameter was often not well controlled in previous experiments.

B. Steady-State Droplet Size of 10%-dispersed Phase Blend

When the 10%- dispersed phase blends were sheared to a sufficiently high strain, a steady-state morphology was obtained, representing a dynamic equilibrium between droplet breakup and coalescence. From images of the steady-state morphology of concentrated blends containing 10% by weight of the dispersed phase, the steady-state volume-averaged droplet diameter (D_v) and steady-state capillary number (Ca_{ss}) calculated from D_v were determined. Figure 3.9 shows that Ca_{ss} increases monotonically with increasing elasticity of the dispersed phase for blends A0, A1, A2, A5, and A10. Figure 3.9 also shows that Ca_{ss} depends on shear rate, even for a nearly Newtonian blend (A0 blend). Possible reasons may include the effect of weak elasticity of the PDMS matrix fluid, or a dependence on shear rate of the critical thickness of the lubricating layer between droplets at which coalescence occurs.

It is also interesting to note that Ca_{ss} obtained from a 10%-dispersed phase blend is smaller than Ca_{crit} obtained from an isolated droplet for the same blend system; that is, the average droplet size in the blend is smaller than the critical size for breakup of an isolated droplet at the same shear rate. This result is initially surprising, since coalescence can occur in the 10% blend, but not for an isolated droplet, and this would tend to make the average droplets bigger in the blends, not smaller, as is actually seen in the experiments. This phenomenon, i.e., droplets in a blend that are smaller on average than the droplet size at which breakup occurs for an isolated droplet at the same shear rate, was previously found when comparing Ca_{ss} of a 20%-dispersed phase blend with Ca_{crit} for an isolated droplet, where both fluids were Newtonian Lerdwijitjarud *et al.* (2003)]. Jansen *et al.* (2001) observed that Ca_{crit} decreases with increasing concentration of dispersed phase. One possible

reason for this phenomenon is that the flow in the blend is locally highly nonuniform and non-steady due to the presence of many other droplets in the vicinity of any one droplet, and this can lead to droplet breakup at a lower average shear rate than occurs for an isolated droplet [Lerdwijitjarud *et al.* (2003)].

We also tried to find a relationship between the degree of droplet elasticity and Ca_{ss} for the blend systems containing 10%-dispersed phase. Since the matrix phase used for all blends is the same pure PDMS, which shows only a very weakly elastic behavior even at high shear rates and its rheological properties do not change much with temperature, the $N_1(\dot{\gamma})$ value of the dispersed phase was chosen to be the index of blend elasticity. Figure 3.10 depicts the correlation between the steady-state capillary number (Ca_{ss}) and N_1 of dispersed phase ($N_{1d}(\dot{\gamma})$) as a semi-logarithmic plot. This plot shows that Ca_{ss} increases monotonically with N_{1d}, which implies that the elasticity of the dispersed phase resists droplet breakup. The scatter in Figure 3.10 indicates that Ca_{ss} may be affected by factors other than N_{1d}, even though all data were obtained at a viscosity ratio of unity. Other factors that might affect Ca_{ss} might include shear thinning, the second normal stress differences of either phase, or the time-dependent elasticity, as well as interactions of these phenomena with coalescence or breakup. While Figure 3.10 does provide a clearer correlation of average droplet size with droplet elasticity under better controlled conditions than has heretofore been achieved, more experiments, and especially numerical simulations of droplet breakup and coalescence for fluids modeled by well defined constitutive equations, will be needed to provide further clarification and more precise correlations.

CONCLUSIONS

We studied the contribution of droplet elasticity to steady-state deformation and breakup of isolated polybutadiene (PBd) droplets in a sheared poly(dimethyl siloxane) (PDMS) matrix fluid and on steady-state droplet size in blends of 10%-dispersed Pbd in PDMS under conditions at which both matrix and droplet fluid has the same viscosity. The steady-state deformation of isolated droplets decreases with increasing dispersed phase elasticity for the same imposed capillary number. A linear relationship between critical capillary number for droplet breakup (Ca_{crit}) and dispersed-phase Weissenberg number (Wi_d) holds up to a value of Wi_d around unity, with a saturation of Ca_{crit} at around $Ca_{crit} = 0.95$ for high Wi_d. The steady-state capillary number (Ca_{ss}) obtained from the average steady-state droplet size in blends containing 10% by weight of dispersed phase is less than the value of Ca_{crit} obtained for an isolated droplet of the same fluid in the same matrix fluid used in the blend. Ca_{ss} is found to increases monotonically with the first normal stress difference of dispersed phase (N_{1d}).

ACKNOWLEDGEMENTS

W.L. and A.S. would like to acknowledge the fellowship provided by Thailand Research Fund (TRF) in the Royal Golden Jubilee Ph D. Program grant no. PHD/00144/2541, and the TRF-BRG grant no. BRG/12/2544.

REFERENCES

Bentley, B.J., and Leal, L.G., "An experimental investigation of drop deformation and breakup in steady, two-dimensional linear flows," *J. Fluid Mech.* **167**, 241-283 (1986).

Boger, D. V. and R. J. Binnington, "Separation of elastic and shear thinning effects in the capillary rheometer", *Trans. Soc. Rheol.* **21**, 515-534 (1977).

Chaffey, C. E. and H. Brenner, "A second-order theory for shear deformation of drops", *J. Colloid Interface Sci.* **24**, 258-269 (1967).

De Bruijn, R. A., "Deformation and breakup of drops in simple shear flow", Ph.D.Thesis, Eindhoven University of Technology, 1989.

Elmendorp, J. J. and R. J. Maalcke, "A study on polymer blending microrheology: Part 1", *Polym Eng. Sci.* **25**, 1041-1047 (1985).

Flumerfelt, R. W."Drop breakup in simple shear fields of viscoelastic fluids", *Ind. Eng. Chem. Fundam.*, **11**, 312-318 (1972).

Grace, H. P., "Dispersion phenomena in high viscosity immiscible fluid systems and application of static mixers as dispersion devices in such systems", *Chem. Eng. Commun.* **14**, 225-277 (1982).

Graebling, D., R. Muller, and J. F. Palierne, "Linear viscoelastic behavior of some incompatible polymer blends in the melt. Interpretation of data with a model of emulsion of viscoelastic liquids", *Macromolecules* **26**, 320-329 (1993).

Guido, S., and M. Villone, "Three-dimensional shape of a drop under simple shear flow", *J. Rheol.* **42**, 395-415 (1998).

Guido, S., and M. Villone. "Measurement of interfacial tension by drop retraction analysis", *J. Colloid and Interface Science* **209**, 247-250 (1999).

Hobbie, E. K. and K. B. Migler, "Vorticity elongation in polymeric emulsions," *Phys. Rev. Lett.* **82**, 5393-5396 (1999).

Jansen, K. M. B., W. G. M. Agterof, and J. Mellema, "Droplet breakup in concentrated emulsions", *J. Rheol.* **45**, 227-236 (2001).

Kennedy, M. R., C. Pozrikidis, and R. Skalak, "Motion and deformation of liquid drops, and the rheology of dilute emulsions in simple shear flow", *Comput. Fluids* **23**, 251-278 (1994).

Lerdwijitjarud, W., R. G. Larson, and A. Sirivat, "Influence of weak elasticity of dispersed phase on droplet behavior in sheared polybutadiene/ poly(dimethylsiloxane) blends," *J. Rheol.* **47**, 37-57 (2003).

Levitt, L., C. W. Macosko and S. D. Pearson, "Influence of normal stress difference on polymer drop deformation", *Polym. Eng. Sci.* **36**, 1647-1655 (1996).

Luciani, A., M. F. Champagne, L. A. Utracki, "Interfacial tension coefficient from the retraction of ellipsoidal drops", *J. Polym. Sci. Pol. Phys.* **35**, 1393-1403 (1997).

Mighri, F., P. J. Carreau, and A. Ajji, "Influence of elastic properties on drop deformation and breakup in shear flow" *J. Rheol.* **42**, 1477-1490 (1998).

Mighri, F. and M. A. Huneault, "Dispersion visualization of model fluids in a transparent Couette flow cell," *J. Rheol.* **45**, 783-797 (2001).

Migler, K. B., "Droplet vorticity alignment on model polymer blends," *J. Rheol.* **44**, 277-290 (2000).

Milliken, W. J., and L. G. Leal, "Deformation and breakup of viscoelastic drops in plannar extensional flows", *J. Non-Newtonian Fluid Mech.* **40**, 355-379 (1991).

Mo, H., C. Zhou, and W. Yu, "A new method to determine interfacial tension from the retraction of ellipsoidal drops", *J. Non-Newtonian Fluid Mech.* **91**, 221-232 (2000).

Okamoto, K., M. Takahashi, H. Yamane, H. Kashihara, H. Watanabe and T. Masuda, "Shape recovery of a dispersed droplet phase and stress relaxation after application of step shear strains in a polystyrene/polycarbonate blend melt", *J. Rheol.* **43**, 951-965 (1999).

Palierne, J. F., "Linear rheology of viscoelatic emulsions with interfacial tension", *Rheol. Acta* **29**, 204-214 (1990).

Rallison J. M., and A. Acrivos, "numerical study of deformation and burst of a viscous drop in an extensional flow", *J. Fluid Mech.* **89**, 191-200 (1978).

Taylor, G. I., "The viscosity of a fluid containing small drops of another fluid", *Proc. R. Soc. London*, Ser. A **138**, 41-48 (1932).

Taylor, G. I., "The formation of emulsions in definable fields of flow", *Proc. R. Soc. London*, Ser. A **146**, 501-523 (1934).

Tretheway D. C., and L. G. Leal, "Deformation and relaxation of Newtonian drops in planar extensional flows of a Boger fluid" *J. Non-Newtonian Fluid Mech.* **99**, 81-108 (2001).

Uijittewaal, W. S. J. and E. J. Nijhof, "The motion of a droplet subjected to linear shear flow including the presence of a plane wall", *J. Fluid Mech.* **302**, 45-63 (1995).

Varanasri, P. P., M. E. Ryan, and P. Stroeve, "Experimental study on the breakup of Model viscoelastic drops in uniform shear flow", *Ind. Eng. Chem. Res.* **33**, 1858-1866 (1994)

Wu, S., "Phase structure and adhesion in plymer blends: A criterion for rubber toughening", *Polymer* **26**, 1855-1863 (1985).

Wu, S., "Formation of Dispered phase in incompatible polymer blends-interfacial and rheological effects." Polym. Eng. Sci. **27**, 335-343 (1987).

Xing, P., M. Bousmina, and D. Rodrigue, "Critical experimental comparison between five techniques for the determination of interfacial tension in polymer blends: model system of polystyrene/polyamide-6", *Macromolecules* **33**, 8020-8034 (2000).

Yamane, H., M. Takahashi, R. Hayashi, K. Okamoto, H. Kashihara and T. Masuda, "Observation of deformation and recovery of poly(isobutylene) droplet in a poly(isobutylene)/poly(dimethyl siloxane) blend after application of step shear strain", *J. Rheol.* **42**, 567-580 (1998).

TABLES

Table 3.1 Properties of materials used

Materials	Molecular Weight (g/mol)	Density at 25 ^{0}C
PDMS	139 000	0.97
PBd	3 900	0.89

Table 3.2 Blend systems studied

Blend	Blend Components (matrix : dispersed)	Testing Temp. (^{0}C)	Γ (mN/m)
A0	PDMS : low-MW PBd	18.3	2.89 ± 0.19
A1	PDMS : 0.1% high-MW PBd solution	19.5	2.80 ± 0.19
A2	PDMS : 0.2% high-MW PBd solution	20.7	2.72 ± 0.22
A5	PDMS : 0.5% high-MW PBd solution	22.0 – 28.0	2.81 ± 0.17 – 2.66 ± 0.28
A10	PDMS : 1.0% high-MW PBd solution	26.0 – 40.0	3.68 ± 0.42 – 2.74 ± 0.13

Table 3.3 The rheological data of blend systems in this studied compared with the data taken from literature.

System	Shear Rate (s^{-1})	Matrix				Droplet				η_r	N_1 ratio (N_{1r})	G' ratio (G'_r)	Ca_1‡	Ca_2§	Ref.
		η*	N_1†	G'	W_i	η	N_1	G'	W_i						
"Boger" Fluids															
A0	1.4	108.1	< 2¶	-	~ 0	108.4	< 1¶	-	~ 0	1.00	-	-	Droplet widening or vorticity stretching is **not** observed.		Lerdwijitjarud *et al* (present work)
A1	1.8	105.3	< 2¶	-	~ 0	104.7	149	-	0.39	0.99	-	-			
A2	1.8	102.6	< 2¶	-	~ 0	100.6	226	-	0.62	0.98	-	-			
A5	2.2	96.4	< 2¶	-	~ 0	92.5	545	-	1.35	0.96	-	-			
A10	3.9	90.9	< 2¶	-	~ 0	86.4	1943	-	3.14	0.95	-	-			
PIB/ PDMS	5	29.7	6.5	-	0.04	17.8	1200	-	13.5	0.60	185	-	-	-	Migler (2000)
	20	29.7	63	-	0.11	17	19200	-	56.5	0.57	305	-	-	7	
	80	27.3	664	-	0.3	16	307200¶	-	240	0.59	462	-	-	7	
D1/M1	4.6	10	Newtonian		-	13	700	-	11.7	1.3	-	-	5.5	-	Mighri and Huneault (2001)
	9	10			-	13	2350¶	-	20.1	1.3	-	-	-	12	
D2/M2	6.4	30	Newtonian		-	10	74490¶	-	1162	0.33	-	-	5.5	-	
	7.7	30			-	10	100000¶	-	1300	0.33	-	-	-	6.5	
D2/M1	48.2	10	Newtonian		-	2	500000¶	-	5185	0.2	-	-	9	-	
Polymer Melts															
PS1/PE2	280	175	288000¶	-	5.88	303	460000¶	-	5.42	1.73	1.60	-	53	-	Hobbie and Migler (1999)
	320	170	300000¶	-	5.51	278	560000¶	-	6.29	1.64	1.87	-	-	60	
PS1/PE1	290	22	41780	-	6.55	288	14497	-	0.17	13	0.35	-	13	-	
	700	14.5	57288	-	5.64	207	31041	-	0.21	14	0.54	-	-	31	
A	0.28	2524	403	135	0.38	2370	205	70	0.21	0.94	0.51	0.52	-	-	Cherdhirankorn *et Al* Submitted to Rheologica acta
	0.3	2505	435	145	0.39	2360	226	78	0.22	0.94	0.52	0.54	-	12	
	0.5	2340	772	250	0.43	2270	468	181	0.32	0.97	0.61	0.72			
	0.8	2170	1310	410	0.47	2133	912	395	0.46	0.98	0.70	0.96	-	-	
B	1.0	603	-	34.2	0.11	619	-	64.7	0.21	1.03	-	1.89	-	28	

* η [=] Pa.s
† N_1, G' [=] Pa
‡ Ca at which droplet first contracts in the vorticity direction
¶ Extrapolated values
§ Ca at which droplet reorients to the vorticity alignment

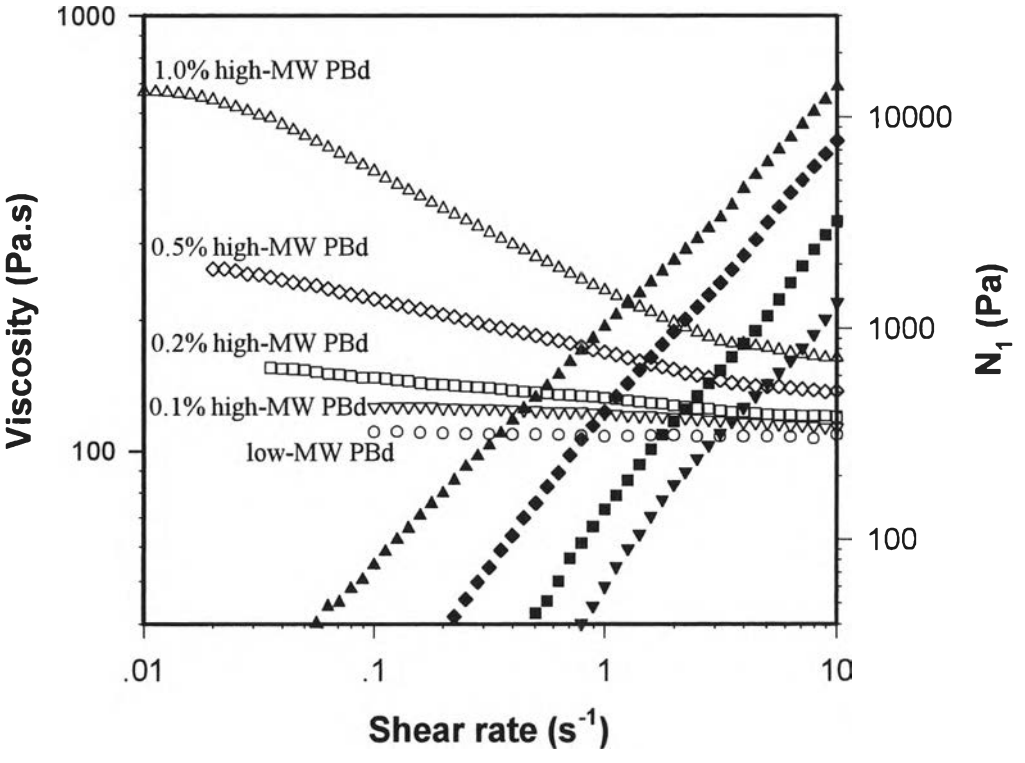

Figure 3.1 The dependence on shear rate of steady-state viscosity (open symbols) and of the first normal stress difference (closed symbols) for low-molecular-weight PBd and PBd "Boger" fluids at 18.3 ^{0}C

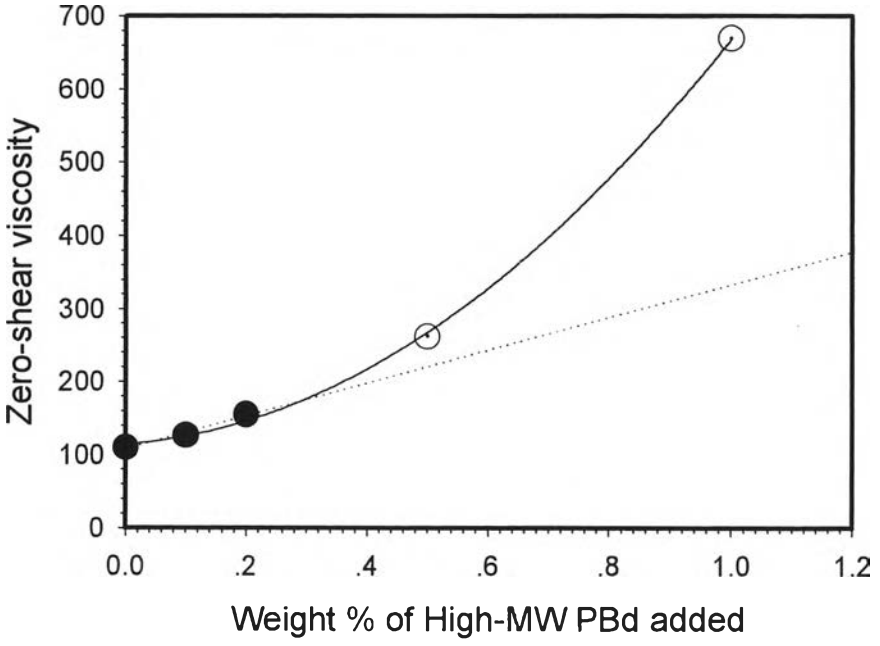

Figure 3.2 The dependence of zero-shear viscosity on the weight percentage of high-molecular-weight PBd added to low molecular-weight Pbd. The filled symbols are in the range where the viscosity depends linearly on concentration

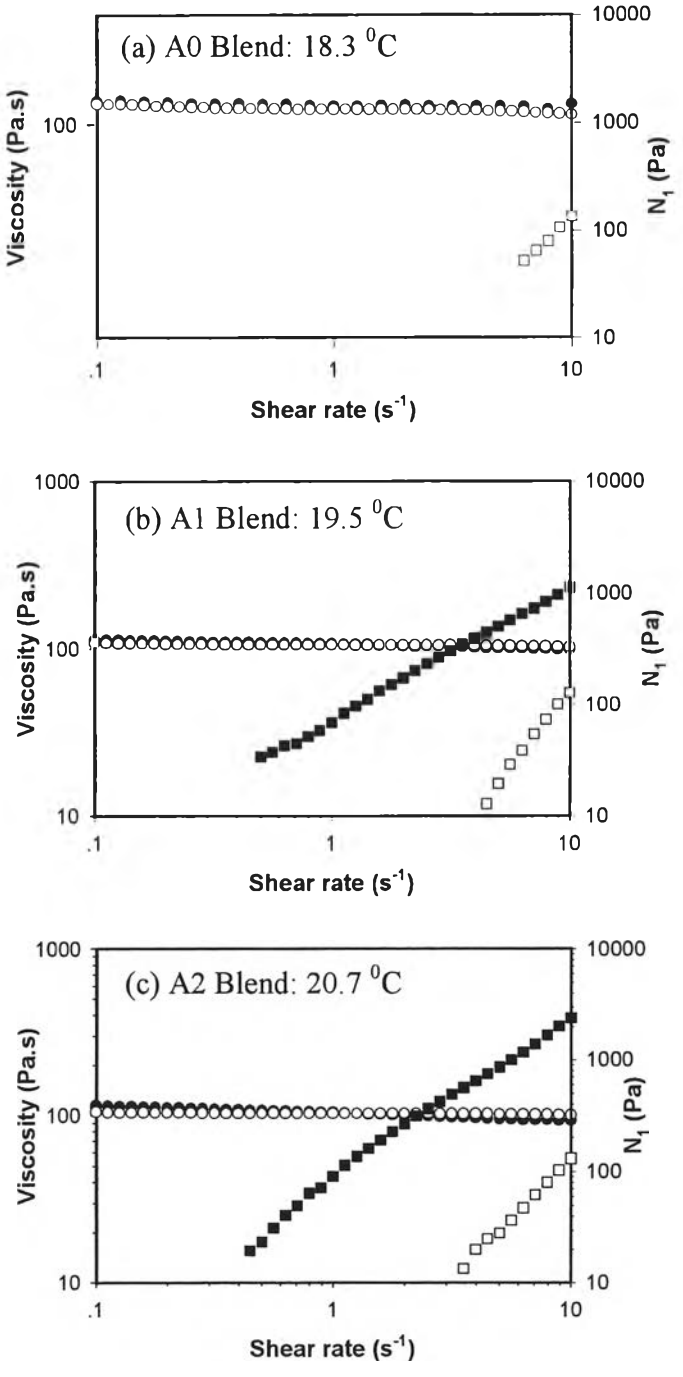

Figure 3.3 The shear-rate dependence of the viscosity of PDMS (O) and of low-molecular-weight PBd or PBd "Boger" fluids (●), as well as the shear-rate dependence of the first normal stress difference of PDMS (□), and of PBd "Boger" fluids (■) for (a) blends A0, (b) A1, and (c) A2 at temperatures chosen such that the PDMS and Pbd fluids have nearly the same viscosity

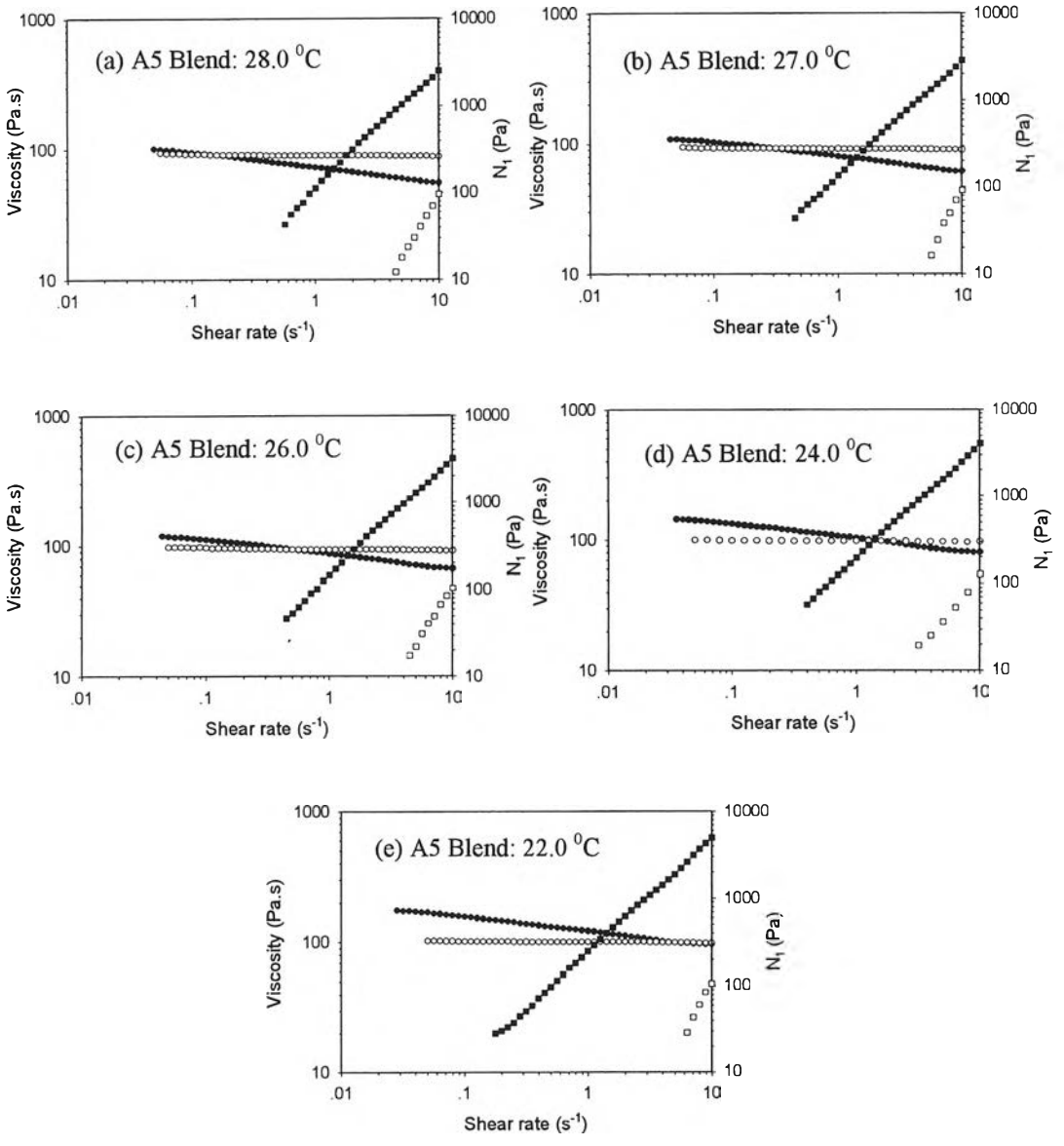

Figure 3.4 The shear-rate dependence of the viscosity of PDMS (O), and of PBd "Boger" fluids (●), and the shear-rate dependence of the first normal stress difference of PDMS (□), and of PBd "Boger" fluid (■) for blend A5 at a series of temperatures

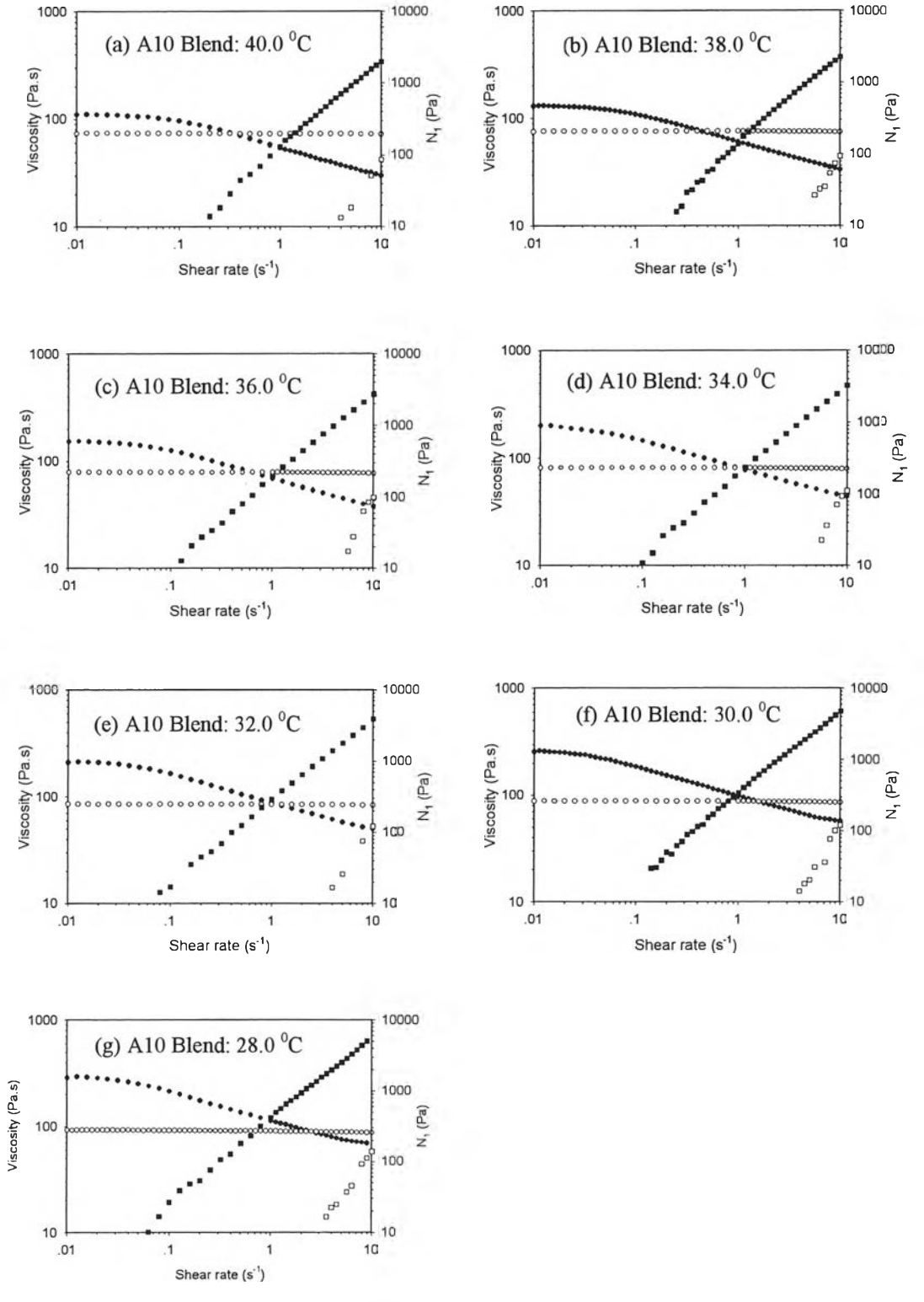

Figure 3.5 The same as Figure 4, except for blend A10

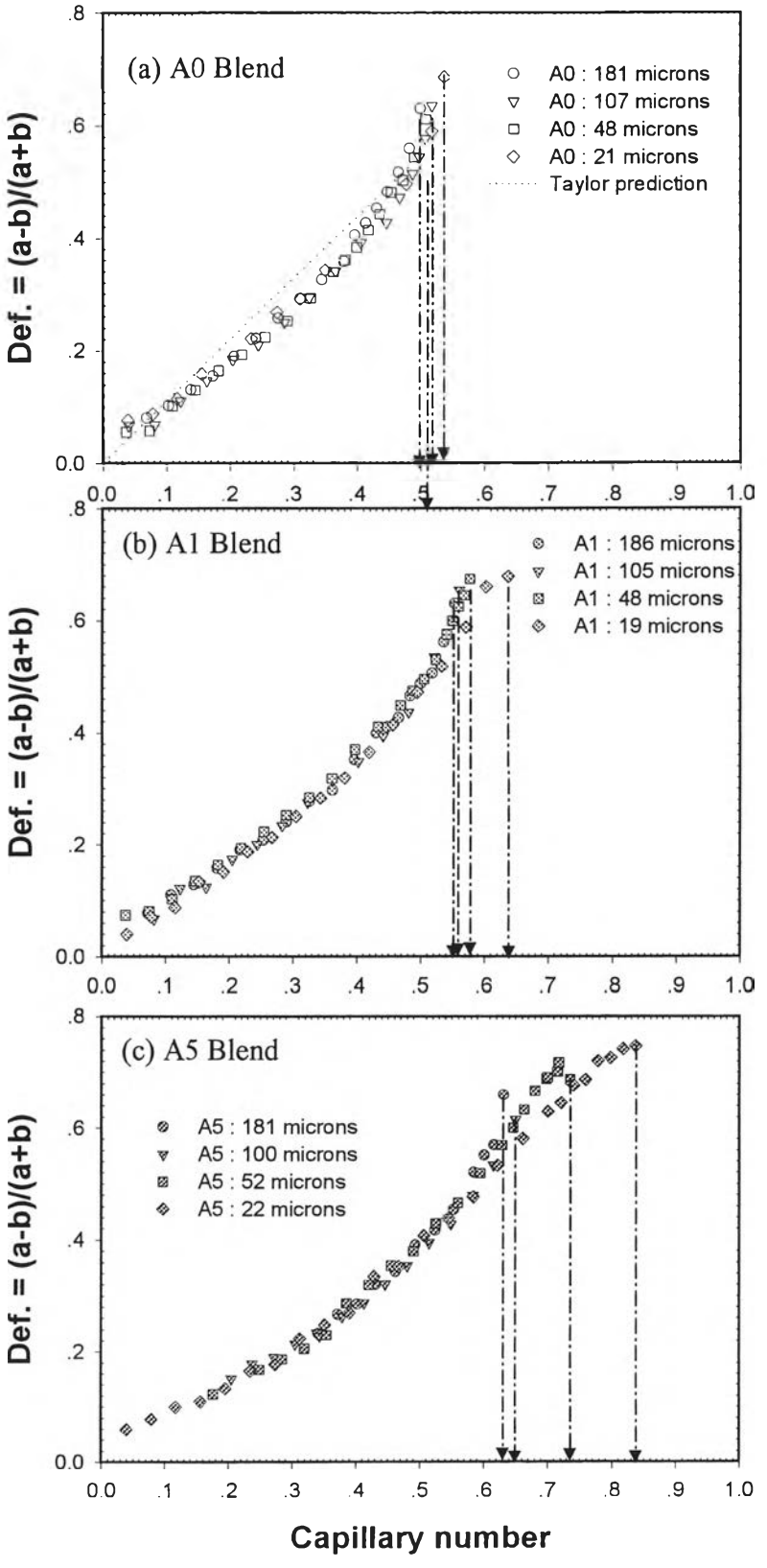

Figure 3.6 The dependence of the deformation parameter on capillary number for blends (a) A0, (b) A1, and (c) A5 for various droplet sizes

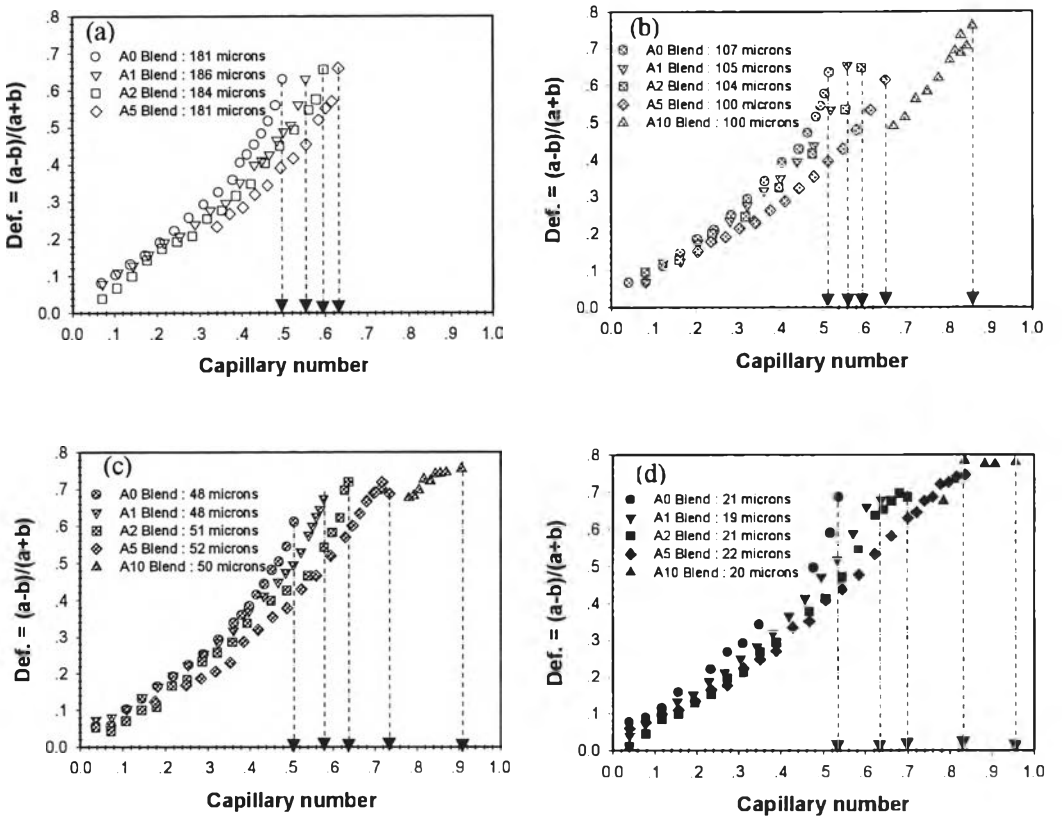

Figure 3.7 The dependence of deformation parameter on capillary number for blends A0, A1, A2, A5, and A10 for droplet diameters of (a) 180μm ± 10%, (b) 100μm ± 10%, (c) 50μm ± 10%, and (d) 20μm ± 10%

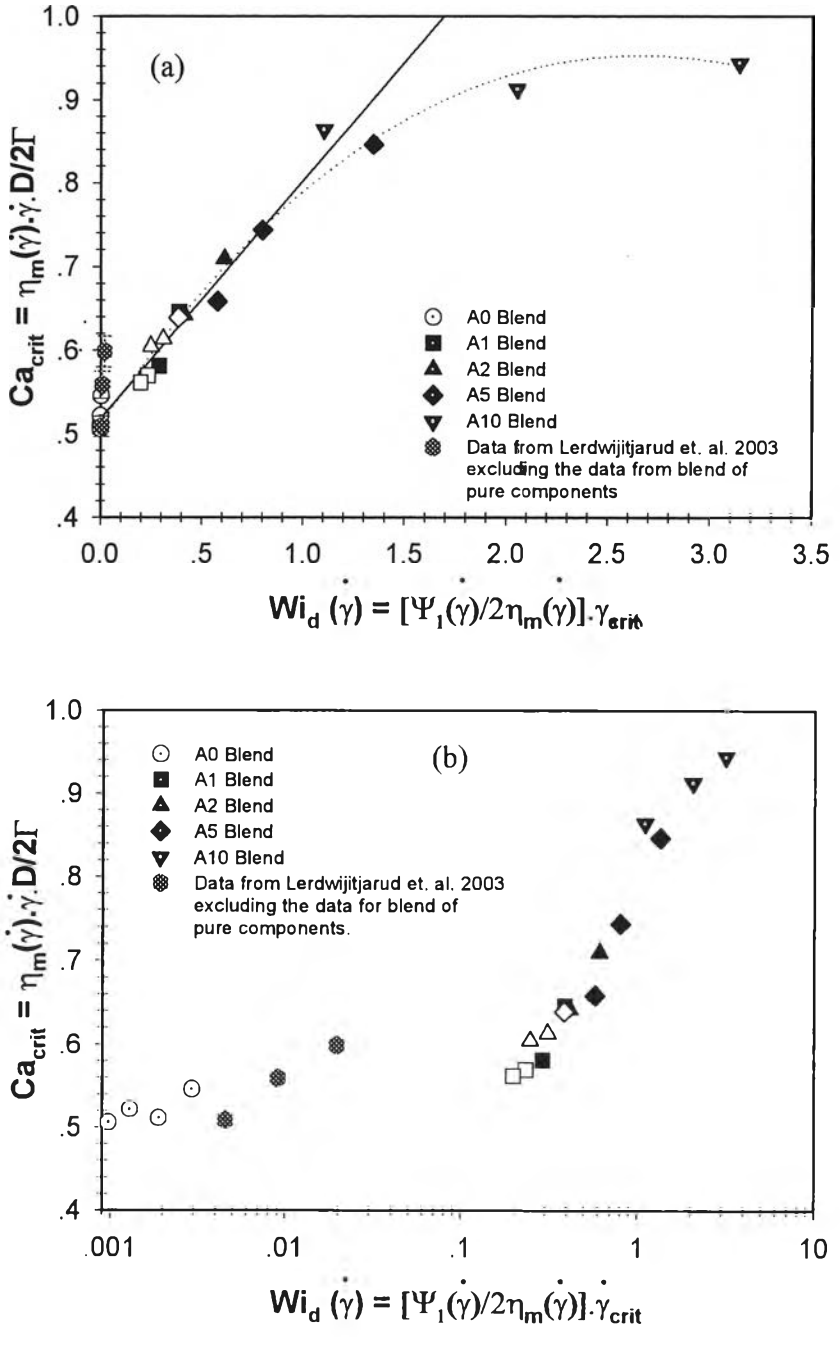

Figure 3.8 The dependence of critical capillary number for droplet breakup (Ca_{crit}) on Weissenberg number of the dispersed phase (Wi_d) (a) linear plot, and (b) semi-log plot. The closed symbols represent the data obtained from the measured N_1 values and the open symbols from extrapolated N_1 values. Data from earlier work (Lerdwijitjarud, et al. 2003) are also included

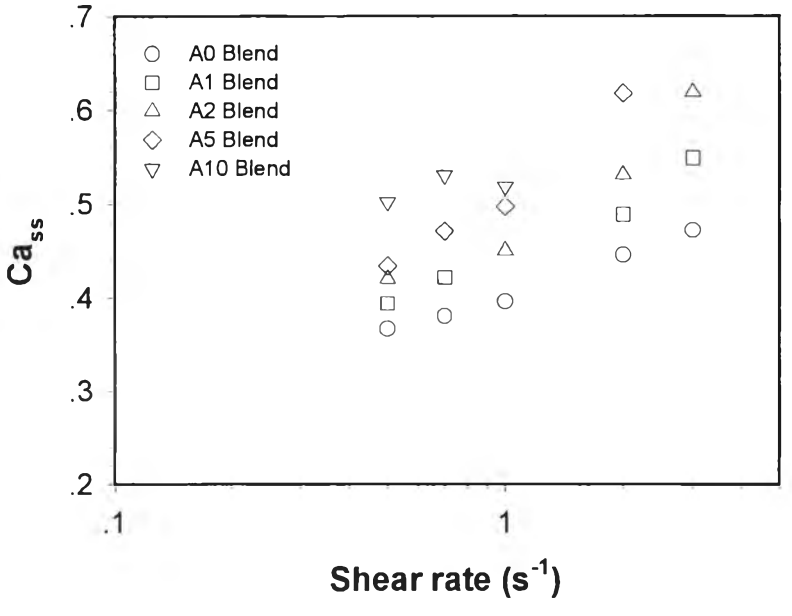

Figure 3.9 The shear-rate dependence of steady-state capillary number (Ca_{ss}) for all 10%-dispersed phase blends studied

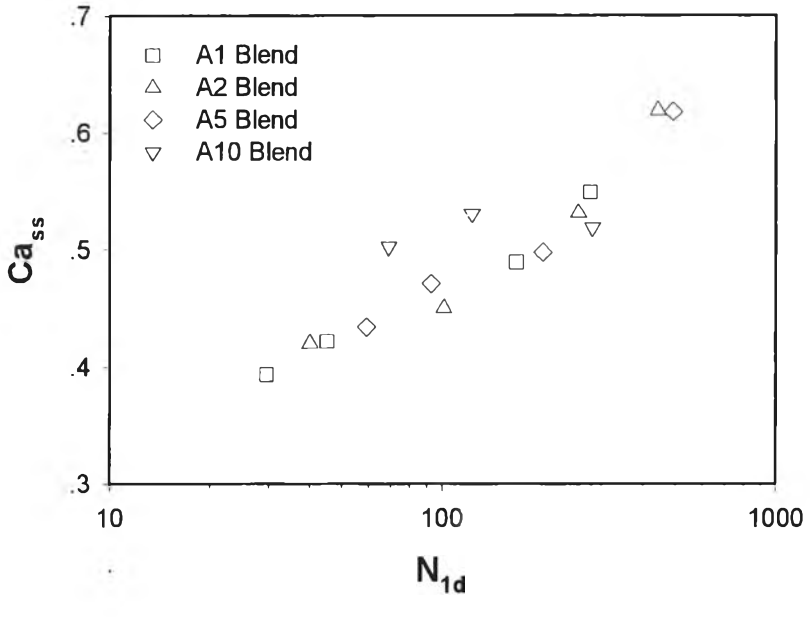

Figure 3.10 The dependence of the steady-state capillary number (Ca_{ss}) on the first normal stress difference of dispersed phase (N_{1d}) for blends A1, A2, A5, and A10